Highly Efficient, Inverted Polymer Solar Cells with Indium Tin Oxide Modified with Solution-Processed Zwitterions as the Transparent Cathode

Kuan Sun,[†] Baomin Zhao,[†] Amit Kumar,[‡] Kaiyang Zeng,[‡] and Jianyong Ouyang*,[†]

[†]Department of Materials Science and Engineering, National University of Singapore, Singapore 117576
[‡]Department of Mechanical Engineering, National University of Singapore, Singapore 117576

ABSTRACT: Polymer solar cells (PSCs) with inverted structure can greatly improve photovoltaic stability. This paper reports a novel method to lower the work function of indium tin oxide (ITO) through the modification with a thin layer of zwitterions which have both positive and negative charges in the same molecule. Zwitterions have a strong dipole moment due to the presence of the two types of charges and are immobile under electric field. Zwitterions with both conjugated and saturated structure were investigated. A zwitterion thin layer is formed on ITO by spin coating a methanol solution of the zwitterion. The zwitterion-modified ITO sheets can be used as the cathode for the electron collection of inverted PSCs. The inverted poly(3-hexylthiophene):[6,6]-phenyl-C61-butyric acid methyl ester (P3HT:PC$_{61}$BM) PSCs can exhibit photovoltaic efficiency as high as 3.98% under simulated AM1.5G illumination (100 mW cm^{-2}), which is comparable to that of PSCs with normal architecture. The effective electron collection by the zwitterion-modified ITO sheets is attributed to the reduction of the work function of ITO as a result of the dipole moment by the zwitterions. The zwitterion modification can lower the work function of ITO by up to 0.97 eV. The photovoltaic performance of PSCs and the reduction in the work function of ITO strongly depend on the chemical structure of the zwitterions.

KEYWORDS: inverted polymer solar cell, ITO modification, work function, zwitterions, dipole
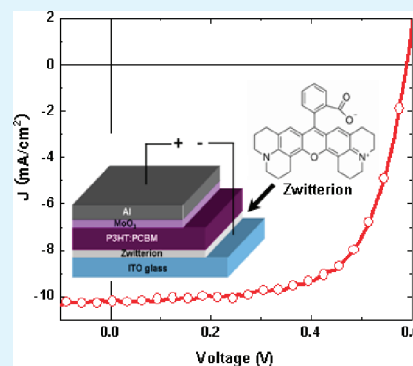
1. INTRODUCTION

Polymer solar cells (PSCs) have been attracting considerable attention. They are regarded as the next-generation solar cell technology due to their low fabrication cost, lightweight, and high mechanical flexibility. Much effort has been devoted to improve the photovoltaic performance, such as the synthesis of new donor or acceptor materials[1−11] and the development of novel processing techniques to manipulate the morphology of the active layer.[12−17] Power conversion efficiency (PCE) of close to 10% has been documented.[18,19] Besides the PCE, the stability is also important for their practical application. Inverted PSCs can greatly improve the stability, because they use neither acidic conducting polymer as the buffer layer for the hole collection nor active metal for the electron collection.[20−23] In an inverted cell, the bottom electrode acts as the cathode for the electron collection, while the top electrode serves as the anode for the hole collection. Indium tin oxide (ITO) is the most popular transparent electrode of PSCs, but ITO has a work function of 4.5−4.7 eV, which matches the energy levels of neither the donor nor the acceptor.[24,25] The challenge in building inverted PSCs lies in effectively lowering the work function of ITO. Several methods have been reported to lower the work function of ITO for the electron collection, including the insertion of an interfacial layer with materials of a low work function, such as TiO$_x$ and ZnO,[26−32] and the surface modication of ITO with Al$_2$O$_3$, PbO, inorganic and organic

salts, and organic self-assembled monolayer (SAM).[33−42] The surface modification can effectively lower the work function of ITO as a result of the dipole moment formed on the ITO surface. However, the photovoltaic performance of the inverted PSCs with oxides like TiO$_x$ and ZnO by the sol−gel process is strongly dependent on the morphology of the oxides, since the nanosized oxides can trap charges. Thus, additional modification of the oxides with a monolayer of organic ligand may be required.[37] A big concern for the modification of ITO with salts is the ion motion under the electric field, which can affect the device performance and deteriorate the device stability.[43,44]

In this paper, we report a novel method to lower the work function of ITO by introducing a thin layer of zwitterions. Zwitterions have positive and negative charges in the same molecule and are immobile under the electric field. The zwitterion layer was formed on ITO by solution processing techniques, such as spin coating of methanol solutions of zwitterions. Zwitterions can lower the work function of ITO by up to 0.97 eV. The zwitterion-modified ITO sheets were used as the cathode for the electron collection. The inverted PSCs with zwitterion-modified ITO as the cathode exhibited a high PCE of 3.98% under simulated AM1.5G illumination (100 mW

cm^{-2}), comparable to that of control PSCs with normal architecture.

2. EXPERIMENTAL SECTION

Materials. Chemical structures of the zwitterions, including *N,N*-dimethyl-*N*-[3-(sulfooxy)propyl]-1-nonanaminium hydroxide (DNSPN), *N*-dodecyl-*N,N*-dimethyl-3-ammonio-1-propanesulfonate (DDMAP), 1-(*N,N*-dimethylcarbamoyl)-4-(2-sulfethyl)pyridinium hydroxide (DMCSP), 4-(triphenylphosphonio)butane-1-sulfonate (TPPBS), 3-(triphenylphosphonio)propane-1-sulfonate (TPPPS), 10-(3-sulfopropyl)acridinium betaine (SPAB), and rhodamine 101,

Scheme 1. Chemical Structures of Zwitterions Used in This Study
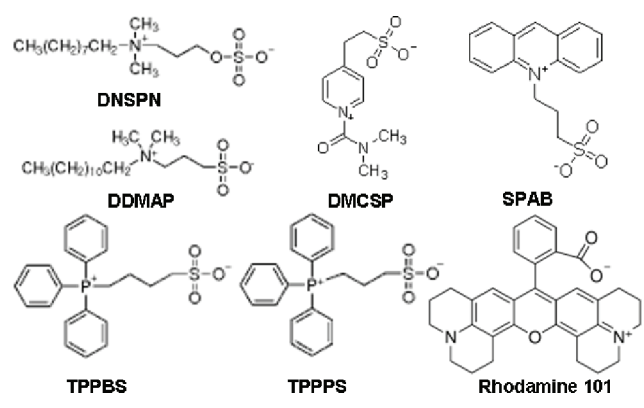
are presented in Scheme 1. They were purchased from Sigma-Aldrich. Regioregular poly(3-hexylthiophene) (P3HT) and (6,6)-Phenyl-C61 butyric acid methyl ester (PC$_{61}$BM) (chemical structures shown in

Scheme 2. (a) Schematic Device Architecture of Inverted PSCs and (b) the Chemical Structure of P3HT and PC$_{61}$BM
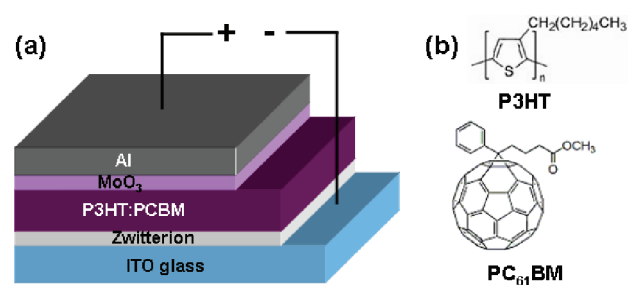
Scheme 2b) were supplied by Rieke Metals and Nano-C, respectively. All other chemicals were obtained from Sigma-Aldrich Co. Ltd. All the chemicals were used without further purification.

Device Fabrication. The inverted PSCs, as illustrated in Scheme 2a, were fabricated through the following process. ITO-coated glass sheets with a surface resistance of 10 Ω sq^{-1} were cleaned sequentially with Decon 90, deionized water, acetone, and isopropyl alcohol. Each cleaning step was carried out in a Branson 1510 ultrasonic water bath for 20 min. The cleaned ITO sheets were dried with nitrogen flow and successively treated by UV-ozone (Jelight 42-220 UVO cleaner) for 15 min. Then, a thin layer of a zwitterion was formed on an ITO sheet by spin coating the methanol solution of the zwitterion at 3000 rpm for 1 min. The zwitterion layer was annealed at 120 °C for 10 min in air. The zwitterion-coated ITO sheets were transferred into a glovebox filled with highly pure nitrogen for the preparation of the active layer. The active layer was deposited by spin coating a dichlorobenzene solution of 20 mg mL^{-1} P3HT and 20 mg mL^{-1} PC$_{61}$BM at 500 rpm for 60 s and subsequently drying at room temperature for 20 min. The

active layer was then annealed at 120 °C for 10 min. Finally, a 7 nm-thick MoO$_3$ layer and a 100 nm-thick Al layer were successively deposited in a chamber of a thermal evaporator at 1 × 10^{-6} mbar. The evaporation rates were 0.1 Å s^{-1} for MoO$_3$ and 2 Å s^{-1} for Al, respectively. The PSCs were encapsulated with UV-curable epoxy glue (Epotek OG112-6 by Epoxy Technology Inc.) and glass sheets in the glovebox. They were taken out of the glovebox for the photovoltaic tests.

Characterizations. Atomic force microscopic (AFM) images were acquired with a Veeco NanoScope IV Multi-Mode AFM system in tapping mode. Surface potential images were collected with a MFP-3D atomic force microscope by Asylum Research in the Kelvin probe force microscopy (KPFM) tapping mode. A Pt-coated cantilever tip (tip radius 15 nm) with a spring constant of 2 N m^{-1} and a resonant frequency of ∼70 kHz (Electric-Lever, Olympus, Japan) were used for the measurement. All of the KPFM measurements are performed at 3 V ac voltage and a lift height of 40 nm under ambient conditions. X-ray photoelectron spectra (XPS) and ultraviolet photoelectron spectra (UPS) were taken with an Axis Ultra DLD X-ray photoelectron spectrometer equipped with an Al Kα X-ray source (1486.6 eV). Contact angles were recorded with a Reme-Hart Contact Angle Goniometer.

The photovoltaic performance of the PSCs was measured with a computer-programmed Keithley 2400 source/meter under a Newport's Oriel class A solar simulator, which simulated the AM1.5 sunlight with energy density of 100 mW cm^{-2} and was certified to the JIS C 8912 standard. The active area of each PSC was 0.11 cm^2.

3. RESULTS AND DISCUSSION

Inverted PSCs with Rhodamine-Modified ITO as Cathode. A zwitterion, also called an inner salt, is a neutral

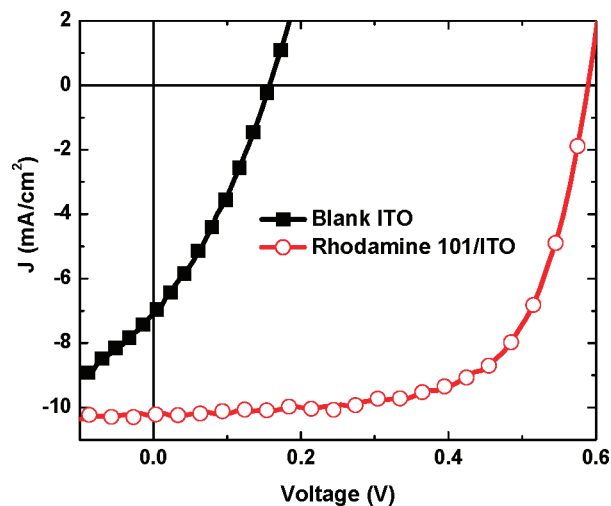**Figure 1.** *J*−*V* curves of inverted PSCs glass/cathode/P3HT:PC$_{61}$BM/MoO$_3$/Al with a blank ITO and a rhodamine 101-treated ITO as the cathode.

Table 1. Photovoltaic Performances of Inverted PSCs Glass/Cathode/P3HT:PC$_{61}$BM/MoO$_3$/Al with (a) a Blank ITO and (b) a Rhodamine 101-Modified ITO as the Cathode

device	V_{oc} (V)	J_{sc} (mA cm^{-2})	FF	best PCE (average)^a (%)	R_s (Ωcm^{-2})	R_{sh} (Ωcm^{-2})
(a)	0.16	7.11	0.31	0.35 (0.31)	7.6	50
(b)	0.59	10.21	0.66	3.98 (3.89)	1.7	29430

^{a}The PCE were averaged over 10 devices. The averaged PCE values are shown in parentheses.

2010

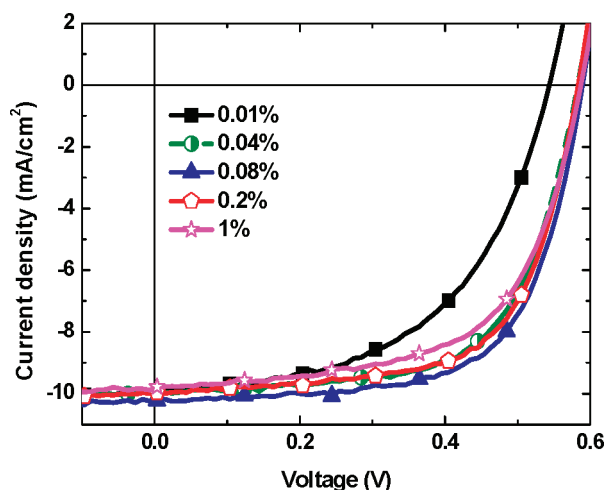dx.doi.org/10.1021/am201844q | *ACS Appl. Mater. Interfaces* 2012, 4, 2009−2017

Figure 2. $J-V$ curves of inverted PSCs glass/ITO/rhodamine 101/P3HT:PC$_{61}$BM/MoO$_3$/Al with the rhodamine 101 layer deposited from the methanol solutions of 0.01, 0.04, 0.08, 0.2, and 1 wt % rhodamine 101.

Figure 3. $J-V$ characteristics of inverted PSCs glass/ITO/zwitterion/P3HT:PC$_{61}$BM/MoO$_3$/Al with different zwitterions.

molecule that possesses both positive and negative charges at different locations of the same molecule. Zwitterions have been used in detergents,[45,46] lithium ion batteries,[47−49] and drug delivery.[50,51] They were also used to increase the conductivity of poly(3,4-ethylenedioxythiophene) poly(styrenesulfonate) (PEDOT:PSS) films.[52] The positive and negative charges form a strong intrinsic dipole moment within the molecule. The zwitterions do not diffuse under an external electrical field. This stimulates us to use zwitterions to modify the surface of ITO.

The zwitterions used in this study are in solid state at room temperature and soluble in polar solvents like methanol. They were used to modify ITO for inverted PSCs whose architecture is shown in Scheme 2a. A thin layer of zwitterions was formed on ITO by spin coating. The thickness of the zwitterion layer was estimated by the optical absorption with the Beer−Lambert law. The active layer of PSCs was prepared by coating a dichlorobenzene solution of P3HT and PC$_{61}$BM. Inverted PSCs with rhodamine 101-modifed ITO exhibited the best photovoltaic performance among the zwitterions in use. The device has a structure of glass/ITO/rhodamine 101/P3HT:PC$_{61}$BM/MoO$_3$/Al. Figure 1 presents the current density (J)−voltage (V) curve of such an inverted PSC. The rhodamine 101 layer was coated from methanol solution of 0.08 wt % rhodamine 101, and its thickness was 1.5 nm. The photovoltaic parameters, including open-circuit voltage (V_{oc}), short-circuit current (J_{sc}), fill factor (FF), and PCE, are summarized in Table 1. The $J-V$ curve of a control inverted PSC with a blank ITO as the cathode is presented as well. The PSC with rhodamine
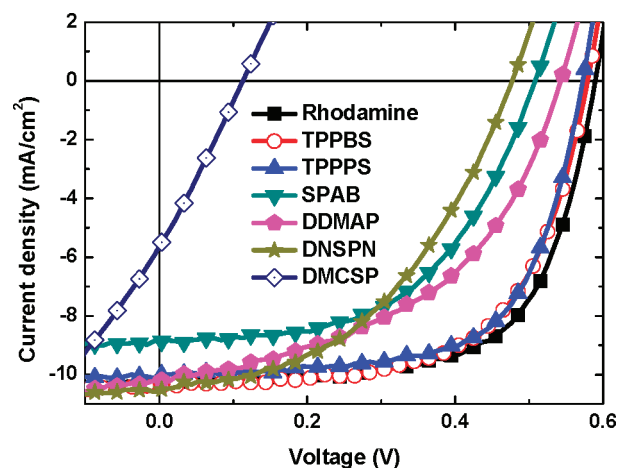
101-modified ITO exhibits high photovoltaic performance. The V_{oc} (0.59 V) and FF (0.66) suggest the efficient electron collection by the modified ITO. The photovoltaic performance is saliently better than that of the control inverted PSC with a blank ITO. The inverted PSC with rhodamine 101-modified ITO has a PCE of 3.98%, while the PCE is only 0.35% for the control device.

The series resistance (R_s) and shunt resistance (R_{sh}) were extracted from the inverse of the slopes of $J-V$ curves of devices in dark at 1 and 0 V, respectively. They are also listed in Table 1. The R_s value of the inverted PSC is much lower than that of the control inverted PSC. It implies that the ITO modification with rhodamine 101 can facilitate the electron transport across the interface between the active layer and ITO. The small R_s value is consistent with the high V_{oc} value.[53] In addition, the R_{sh} value of the inverted PSC is much greater than that of the control inverted PSC. The R_s and R_{sh} values are in good agreement with the photovoltaic performance of the two inverted PSCs.

The photovoltaic performance of the inverted PSC with rhodamine 101-modified ITO cathode depends on the thickness of the rhodamine 101 layer. Figure 2 and Table 2 present the photovoltaic performances of inverted PSCs with rhodamine 101 layer prepared from methanol solutions of different rhodamine 101 concentrations. The thicknesses of rhodamine 101 layers are also presented in Table 2. The inverted PSCs exhibited high photovoltaic performance for the rhodamine 101 concentration varied from 0.04 wt % to 0.2 wt %, and the highest PCE was obtained at 0.08 wt % rhodamine 101. The variations of R_s and R_{sh} of the PSCs with the thicknesses of the rhodamine 101 layer are consistent with photovoltaic performance.

Table 2. Photovoltaic Performances of Inverted PSCs Glass/ITO/Rhodamine 101/P3HT:PC$_{61}$BM/MoO$_3$/Al with the Rhodamine 101 Layer Deposited from the Methanol Solutions of Different Rhodamine 101 Concentrations

conc (%)	thickness (nm)	V_{oc} (V)	J_{sc} (mA cm^{-2})	FF	best PCE (average)^a (%)	R_s (Ωcm^{-2})	R_{sh} (Ωcm^{-2})
0.01	0.3	0.55	9.93	0.53	2.89 (2.61)	3.0	11 160
0.04	0.8	0.59	10.01	0.63	3.72 (3.60)	4.9	17 610
0.08	1.5	0.59	10.21	0.66	3.98 (3.89)	1.7	29 430
0.2	4.0	0.59	9.96	0.65	3.82 (3.67)	1.9	83 260
1.0	16.4	0.59	9.79	0.61	3.52 (3.43)	2.9	154 800

^{a}The PCE were averaged over 10 devices. The averaged PCE values are shown in parentheses.

2011

dx.doi.org/10.1021/am201844q | ACS Appl. Mater. Interfaces 2012, 4, 2009−2017

Table 3. Photovoltaic Performances of Inverted PSCs Glass/ITO/Zwitterion/P3HT:PC$_{61}$BM/MoO$_3$/Al with Different Zwitterions

zwitterion	V_{oc} (V)	J_{sc} (mA cm^{-2})	FF	best PCE (average)^a (%)	R_s (Ωcm^{-2})	R_{sh} (Ωcm^{-2})
rhodamine 101	0.59	10.21	0.66	3.98 (3.89)	1.7	29 430
TPPBS	0.58	10.29	0.63	3.80 (3.63)	1.7	24 180
TPPPS	0.58	10.00	0.65	3.77 (3.59)	2.1	38 290
DDMAP	0.55	10.20	0.48	2.69 (2.57)	5.2	20 410
SPAB	0.52	9.67	0.52	2.58 (2.38)	4.2	22 650
DNSPN	0.47	10.51	0.46	2.27 (2.14)	11.1	14 420
DMCSP	0.22	7.90	0.34	0.59 (0.49)	20.0	90

^{a}The PCE were averaged over 10 devices. The averaged PCE values are shown in parentheses.

Table 4. Contact Angles of a Water Droplet on ITO Sheets Modified with Various Zwitterions

zwitterion	contact angle (°)	zwitterion	contact angle (°)
	8−9	TPPPS	25−26
rhodamine 101	39−40	DNSPN	5−6
TPPBS	36−37	DDMAP	7−8
SPAB	35−36	DMCSP	NA^a

^{a}The contact angle is too small to be measurable.

Inverted PSCs with ITO Sheets Modified with Other Zwitterions. To explore the relationship between the chemical structure of zwitterions and photovoltaic performance of the inverted PSCs, other zwitterions, including DNSPN, DDMAP, DMCSP, TPPBS, TPPPS, and SPAB, were also used to modify ITO. Their chemical structures are presented in Scheme 1. In terms of the chemical structure, these zwitterions can be classified into two groups. The first group includes rhodamine 101, TPPBS, TPPPS, and SPAB, in which the nitrogen or phosphorus atom with the positive charge is connected with bulky aromatic ring(s). The second group includes DNSPN, DDMAP, and DMCSP. Though the nitrogen atom with the positive charge is connected with a benzene ring for DMCSP, it is classified into the second group because the benzene ring is
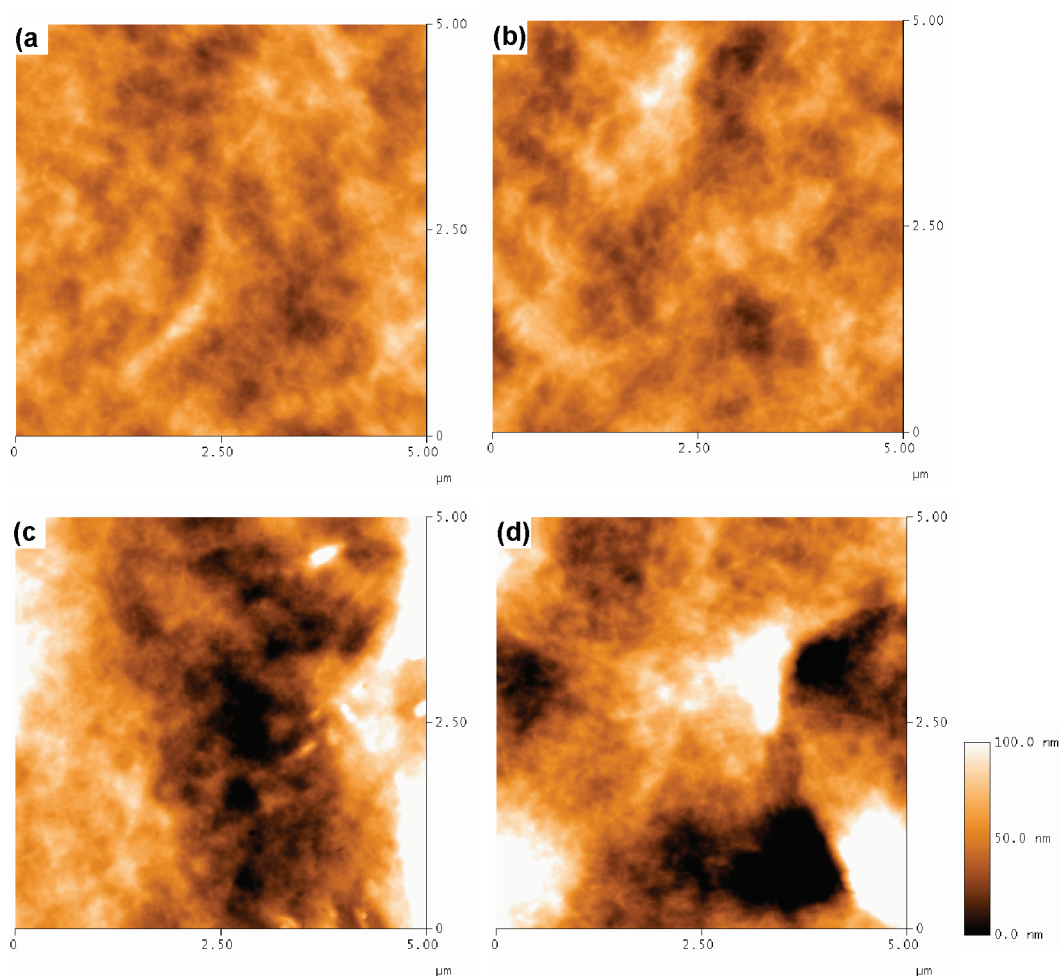

Figure 4. AFM images of P3HT:PC$_{61}$BM films deposited on ITO sheets modified with (a) rhodamine 101, (b) TPPBS, (c) DNSPN, and (d) DMCSP. The image size is 5 um and height bar is 100 nm. The rms roughness values are 11.3, 12.8, 30.5, and 33.8 nm, respectively.
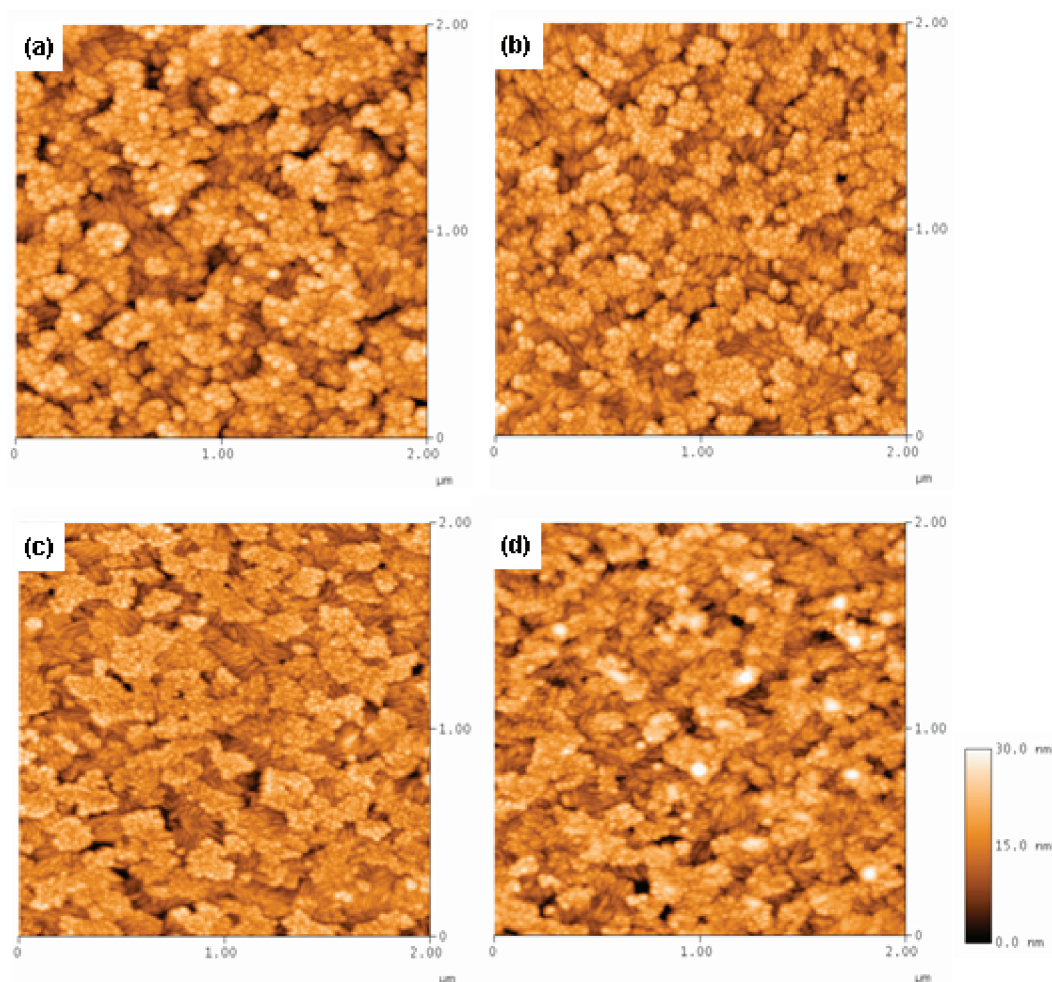
Figure 5. AFM images of (a) a blank ITO and ITO sheets modified by (b) rhodamine, (c) TPPPS, and (d) TPPBS zwitterions. The image size is 2 um and height bar is 30 nm.

less bulky than the aromatic ring(s) of the zwitterions in the first group. The zwitterions are classified in this way because the charge transport through a conjugated structure is significantly different from that through a nonconjugated structure, and the bulky aromatic ring(s) can affect the interactions among the zwitterion molecules.

The ITO sheets were modified with other zwitterions through a similar process as that for rhodamine 101. The optimal concentrations for the photovoltaic efficiency of the inverted PSCs are different for different zwitterions. The optimal concentrations for DNSPN, DDMAP, DMCSP, TPPBS, TPPPS, and SPAB are 0.2, 1, 1, 0.07, 0.02, and 0.5 wt %, respectively. Figure 3 shows the $J-V$ curves of the inverted PSCs with ITO modified with the zwitterion layer prepared from the methanol solutions of optimal zwitterion concentrations. The photovoltaic parameters are listed in Table 3.

The photovoltaic performance of the inverted PSCs is strongly dependent on the chemical structure of the zwitterions. The zwitterions in the first group, particularly rhodamine 101, TPPBS, and TPPPS, give rise to high PCEs, while the zwitterions in the second group lead to low PCEs. The inverted PSCs with DMCSP exhibit the lowest PCE of only 0.59%. The PCE values of the inverted PSCs are generally consistent with their V_{oc} values. This suggests that the surface properties of the zwitterion-modified ITO is the dominant

factor for the photovoltaic performance. As shown in Table 3, the inverted PSCs with rhodamine 101 exhibit the highest fill factor and lowest R_s value. These can be attributed to the conjugated molecular structure that gives rise to a small resistance for the charge transport from the active film into ITO. TPPBS and TPPPS have almost the same chemical structure, except that TPPBS has one more C atom between SO_3^- and P^+. A longer connector can increase the dipole moment, but it also reduces the charge tunneling probability through the zwitterion layer. The inverted PSCs with TPPBS and TPPPS exhibit close photovoltaic performance. Thus, the photovoltiac performance is insensitive to the slight change in the separation between the positive and negative charges. The inverted PSCs with zwitterions of the second group exhibit lower FF and lower R_{sh} values than that with zwitterions of the first group.

The variation of the R_{sh} value with these zwitterions agrees with that of the contact angles of water on zwitterion-modified ITO sheets (Table 4). The contact angle was 8−9° for water on blank ITO which was sequentially cleaned with detergent, water, acetone, and isopropyl alcohol and then treated with UV ozone. It is comparable to the contact angles of UV ozone-treated ITO sheets reported in literature.[54,55] The contact angle increases after the modification with the zwitterions of the first group, whereas it decreases after the modification with the zwitterions of the second group. In other words, the zwitterions
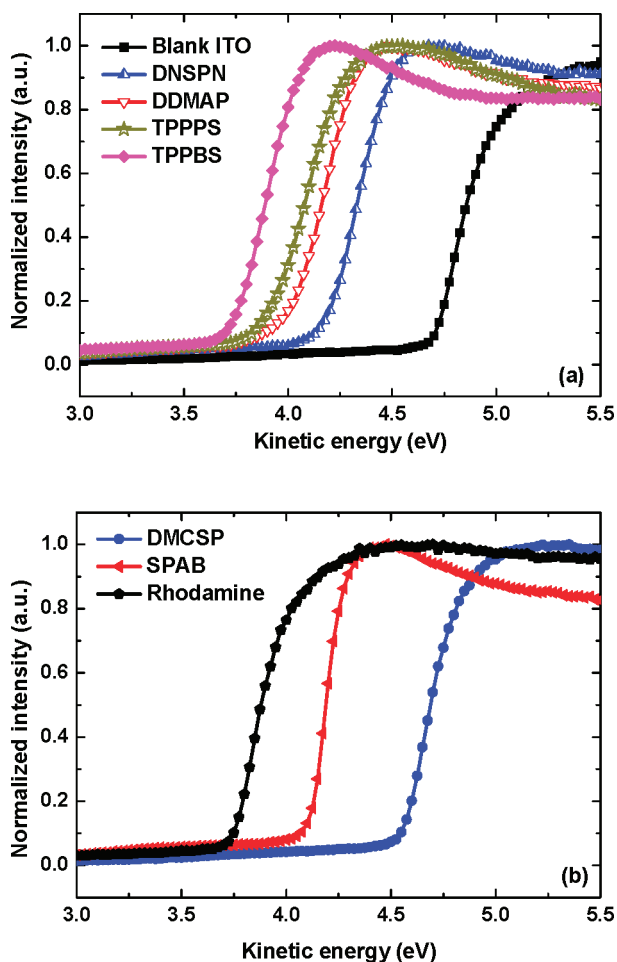
Figure 6. Normalized UPS spectra of a blank ITO and ITO sheets modified with various zwitterions.

Table 5. Effective Work Functions (Φ) of ITO Sheets Modified with Various Zwitterions[a]

zwitterion	Φ (eV)	$\Delta\Phi$ (eV)	zwitterion	Φ (eV)	$\Delta\Phi$ (eV)
	−4.69	0	SPAB	−4.00	0.69
DMCSP	−4.54	0.14	TPPPS	−3.90	0.79
DNSPN	−4.17	0.52	rhodamine 101	−3.73	0.96
DDMAP	−4.12	0.57	TPPBS	−3.72	0.97

[a] $\Delta\Phi$ values are for the reductions in the work function.

of the first group make the ITO surface more hydrophobic, whereas the zwitterions of the second group turn the ITO
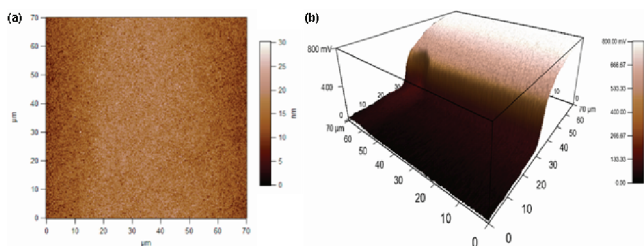

Figure 7. (a) Topography and (b) 3D surface potential of an ITO sheet partially covered with 1 nm-thick rhodamine 101 film deposited by thermal evaporation. The dimension is 70 um. The scale bars are 30 nm and 800 mV for topography and surface potential, respectively.

surface to be more hydrophilic. This implies that the zwitterions can affect the morphology of the active layer of PSCs. The surface morphology of P3HT:PC$_{61}$BM films on ITO sheets coated with rhodamine 101, TPPBS, DNSPN, and DMCSP was studied by AFM (Figure 4). The P3HT:PC$_{61}$BM films are smooth on rhodamine 101 and TPPBS-modified ITO sheets, while those on DNSPN and DMCSP-treated ITO sheets are quite rough. The rms roughness values of the P3HT:PC$_{61}$BM films are 11.3, 12.8, 30.5, and 33.8 nm for ITO sheets modified with rhodamine 101, TPPBS, DNSPN, and DMCSP, respectively. The different roughness values of the active films can be attributed to the differences in the hydrophilicity of the ITO surfaces with different zwitterions. The relative hydrophobic ITO surfaces with the zwitterions of the first group give rise to smooth active films, while the hydrophilic ITO surfaces with the zwitterions of the second group lead to rough active films.

The effect of the zwitterions on the morphology of the active P3HT:PC$_{61}$BM film is due to the hydrophilicity/hydrophobicity of the ITO surface rather than the morphology of the modified ITO sheets. Zwitterions do not have remarkable effect on the morphology of the ITO surface. Figure 5 presents the AFM images of a blank ITO sheet and ITO sheets modified with rhodamine 101, TPPPS, and TPPBS. There is almost no detectable change in the morphology after the zwitterion modification. The rms roughness values of these zwitterion-modified ITO sheets are 4.7, 4.2, 4.4, and 4.6 nm, respectively.

Mechanism for Zwitterion-Induced Reduction in the Work Function of ITO. The work function of zwitterion-modified ITO sheets was investigated by UPS. The cutoff edges are shown in Figure 6. The work function values were summarized in Table 5. TPPBS and rhodamine 101 produce the significant reductions in the work function of ITO by 0.97 and 0.96 eV, respectively. The change in the work function is comparable to the modification of ITO with organic SAMs as reported by Kim et al.[36] In contrast, DMCSP gives rise to a slight reduction in the work function of ITO by only 0.16 eV. The zwitterion-induced change in the work function of ITO is consistent with photovoltaic performance of the inverted PSCs.

The zwitterion-induced change in the work function of ITO was further studied by KPFM.[19] The tests were performed on ITO sheets partially covered with a 1 nm-thick rhodamine 101 layer. The topography and surface potential of ITO were presented in Figure 7a,b. Though the topography change from the uncovered part to the part covered with the rhodamine 101 is not remarkable, the surface potential increases abruptly by 800 mV at the edge from the uncovered ITO part to the part covered with rhodamine 101.

Presumably, the zwitterion molecules chemically adsorb on the ITO surface through the bond formed between the anions, including $-COO^-$, $-SO_3^-$, and $-SO_4^-$, of the zwitterions and ITO.[35,56−58] The interactions between the zwitterions and ITO were investigated by XPS. Figure 8 presents the In 3d and Sn 3d XPS spectra of a blank ITO and ITO sheets modified with various zwitterions. The XPS doublets of both In 3d and Sn 3d shift to red after the zwitterion modification. The red shifts suggest the chemical adsorption of the zwitterions on ITO. Interestingly, the red shift of the binding energy is consistent with the pK_a values of the acids corresponding to the anions of these zwitterions. The pK_a values are 4.76, −1.92, and −3.4 for CH_3COOH, CH_3SO_3H, and CH_3SO_4H, respectively.[59] Thus, a zwitterion with an anion corresponding to a greater pK_a value can bind more strongly to the ITO surface. This phenomenon

2014

dx.doi.org/10.1021/am201844q | *ACS Appl. Mater. Interfaces* 2012, 4, 2009−2017
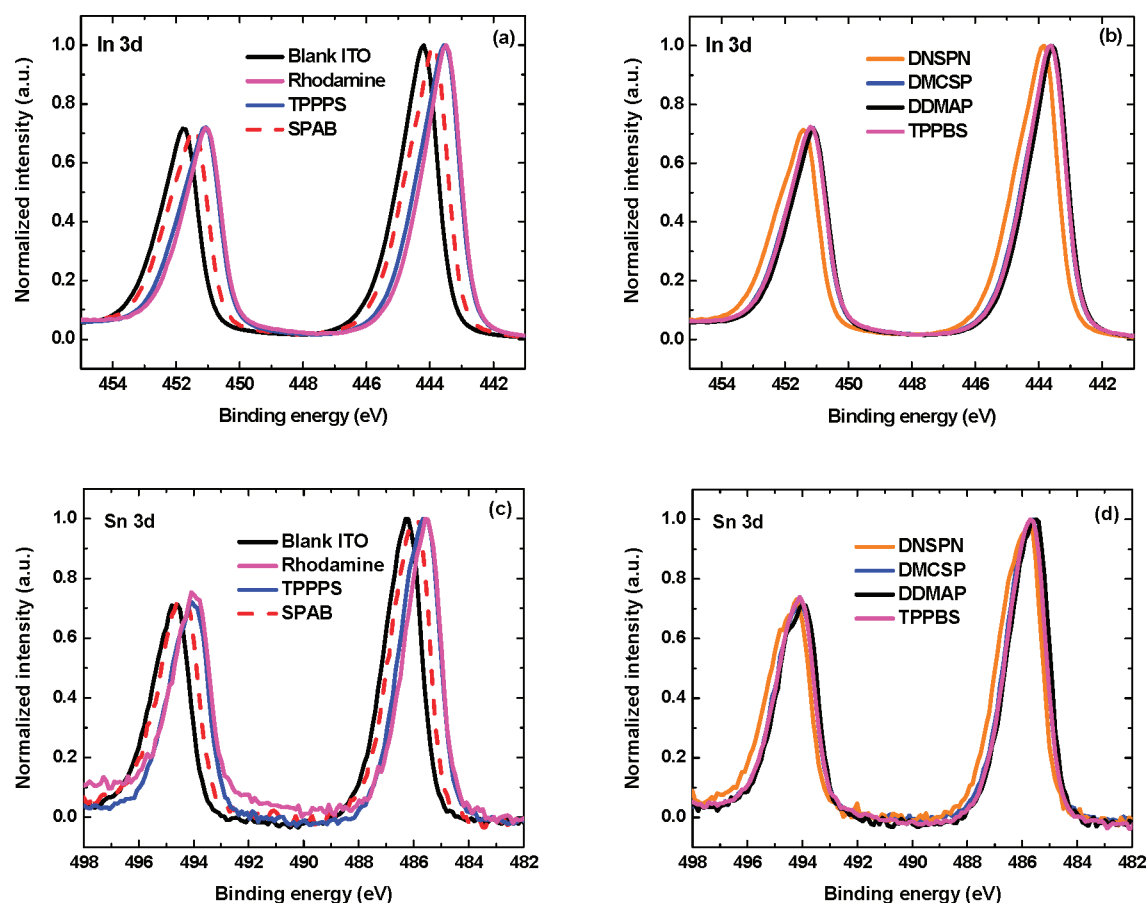
Figure 8. (a, b) In 3d and (c, d) Sn 3d XPS spectra of blank ITO and ITO treated with various zwitterions.

Scheme 3. Schematic (a) Perpendicular and (b) Lie-Down Orientations of Zwitterions on ITO Surface
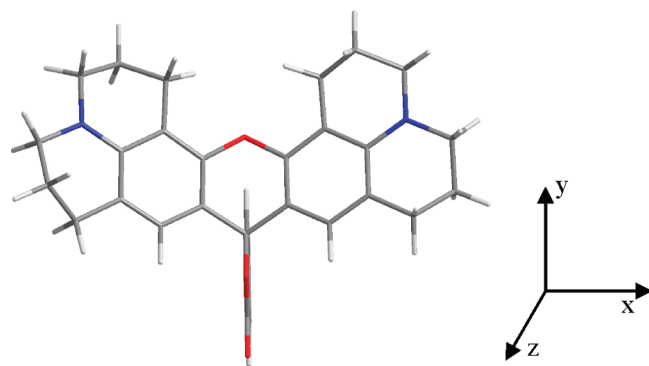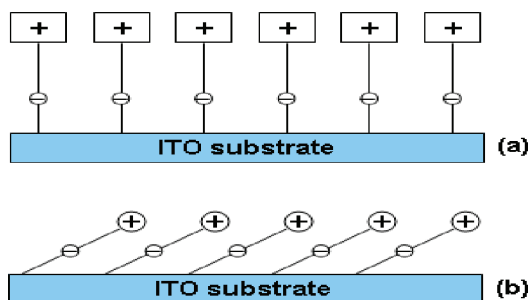

Figure 9. Molecular structure of rhodamine 101 using the Gaussian 03 program.

is in good agreement with our previous study of the ITO modification with sodium compounds.[40]

The different changes in the work function of ITO modified with different zwitterions suggest that the zwitterions have different orientations on the ITO surface. The change in the work function of ITO should be related to the orientation of the dipole moment of the zwitterions on the ITO surface. If all the zwitterion molecules orient perpendicular to the ITO surface as schematically shown in Scheme 3a, the work function change should be similar for all the zwitterions because they have almost the same dipole moment. The work function of ITO changes less remarkably if the zwitterion molecules lie down on the surface of ITO (Scheme 3b). Thus, the zwitterions of the first group likely take the former orientation on ITO, whereas the zwitterions of the second group adopt the latter orientation. The chemical structure of rhodamine 101 was simulated using Gaussian 03 program with the B3LYP-3-21G base set. As shown in Figure 9, the dimensions of the molecule are 13.7, 9.5, and 5.5 Å along x, y, and z directions, respectively. Thus, at the optimal thickness of 1.5 nm, the rhodamine 101 layer consists of 2 or 3 monolayers of rhodamine 101 molecules.

These two pictures for the different orientations of the two groups of zwitterions can account for the contact angles of water on the surface of ITO sheets modified with zwitterions (Table 4). Water exhibits a very small contact angle on ITO modified with the zwitterions of the second group, despite that these zwitterions have a long alkyl chain that should give rise to a hydrophobic surface. In contrast, the surfaces of ITO sheets modified by the zwitterions of first group are more hydro-

phobic. Since the alkyl chains are nonpolar and hydrophobic, the contact angle data suggest the zwitterion molecules of the second group lie down on the ITO surface. Probably, this is due to the strong Coulombic repulsion arising from the charges of the zwitterion molecules. The zwitterions of the first group can orient more perpendicularly on the surface of ITO due to the bulky aromatic ring(s). The bulky aromatic ring(s) gives rise to a remarkable separation for the charges on different molecules. This can reduce the Coulombic repulsion among the zwitterion molecules. In addition, the $\pi-\pi$ overlapping among aromatic ring(s) of zwitterion molecules provides counterforce against the Coulombic repulsion.

4. CONCLUSIONS

In summary, the work function of ITO can be significantly reduced through the modification with zwitterions. The zwitterion-modified ITO sheets were used as the cathode for the electron collection of inverted PSCs. High photovoltaic performance has been observed on the inverted PSCs. The reduction in the work function of ITO and the photovoltaic performance of the inverted PSCs depend on the chemical structure of the zwitterions. Zwitterions with bulky aromatic ring(s) can orient perpendicularly on the ITO and give rise to significant reduction in the work function, because the bulky aromatic ring(s) can reduce the Coulombic repulsion arising from the charges of the zwitterion molecules and give rise to $\pi-\pi$ interactions among the zwitterion molecules.

■ AUTHOR INFORMATION

Corresponding Author
*E-mail: mseoj@nus.edu.sg.

Notes
The authors declare no competing financial interest.

■ ACKNOWLEDGMENTS

■ REFERENCES

(1) Liang, Y.; Xu, Z.; Xia, J.; Tsai, S.-T.; Wu, Y.; Li, G.; Ray, C.; Yu, L. *Adv. Mater.* **2010**, *22*, E135.
(2) Zhou, H.; Yang, L.; Stuart, A. C.; Price, S. C.; Liu, S.; You, W. *Angew. Chem.* **2011**, *123*, 3051.
(3) Huo, L.; Zhang, S.; Guo, X.; Xu, F.; Li, Y.; Hou, J. *Angew. Chem., Int. Ed.* **2011**, *50*, 9697.
(4) Wang, E.; Wang, L.; Lan, L.; Luo, C.; Zhuang, W.; Peng, J.; Cao, Y. *Appl. Phys. Lett.* **2008**, *92*, 033307.
(5) Siddiki, M. K.; Li, J.; Galipeau, D.; Qiao, Q. Q. *Energy Environ. Sci.* **2010**, *3*, 867.
(6) Chu, T.-Y.; Lu, J.; Beauqré, S.; Zhang, Y.; Pouliot, J. R.; Wakim, S.; Zhou, J.; Lecterc, M.; Li, Z.; Ding, J.; Tao, Y. *J. Am. Chem. Soc.* **2011**, *133*, 4250.
(7) Price, S. C.; Stuart, A. C.; Yang, L.; Zhou, H.; You, W. *J. Am. Chem. Soc.* **2011**, *133*, 4625.
(8) Wu, Z.; Fan, B.; Xue, F.; Adachi, C.; Ouyang, J. *Sol. Energy Mater. Sol. Cells* **2010**, *94*, 2230.
(9) Wu, Z.; Fan, B.; Li, A.; Xue, F.; Ouyang, J. *Org. Electron.* **2011**, *12*, 993.
(10) Wu, Z.; Li, A.; Fan, B.; Xue, F.; Adachi, C.; Ouyang, J. *Sol. Energy Mater. Sol. Cells* **2011**, *95*, 2516.
(11) He, Y.; Chen, H.-Y.; Hou, J.; Li, Y. *J. Am. Chem. Soc.* **2010**, *132*, 1377.
(12) Shaheen, S. E.; Brabec, C. J.; Sariciftci, N. S.; Padinger, F.; Fromherz, T.; Hummelen, J. C. *Appl. Phys. Lett.* **2001**, *78*, 841.
(13) Chen, L. M.; Hong, Z.; Li, G.; Yang, Y. *Adv. Mater.* **2009**, *21*, 1434.
(14) Peet, J.; Kim, J. Y.; Coates, N. E.; Ma, W. L.; Moses, D.; Heeger, A. J.; Bazan, G. C. *Nat. Mater.* **2007**, *6*, 497.
(15) Ouyang, J.; Xia, Y. *Sol. Energy Mater. Sol. Cells* **2009**, *93*, 1592.
(16) Ayzner, A. L.; Tassone, C. J.; Tolbert, S. H.; Schwartz, B. J. *J. Phys. Chem. C* **2009**, *113*, 20050.
(17) Moon, J. S.; Takacs, C. J.; Sun, Y.; Heeger, A. J. *Nano Lett.* **2011**, *11*, 1036.
(18) Service, R. F. *Science* **2011**, *332*, 293.
(19) He, Z.; Zhong, C.; Huang, X.; Wong, W.-Y.; Wu, H.; Chen, L.; Su, S.; Cao, Y. *Adv. Mater.* **2011**, *23*, 4636.
(20) Glatthaar, M.; Niggemann, M.; Zimmermann, B.; Lewer, P.; Riede, M.; Hinsch, A.; Luther, J. *Thin Solid Films* **2005**, *491*, 298.
(21) Li, G.; Chu, C.-W.; Shrotriya, V.; Huang, J.; Yang, Y. *Appl. Phys. Lett.* **2006**, *88*, 253503.
(22) Campoy-Quiles, M.; Ferenczi, T.; Agostinelli, T.; Etchegoin, P. G.; Kim, Y.; Anthopoulos, T. D.; Stavrinou, P. N.; Bradley, D. D. C.; Nelson, J. *Nat. Mater.* **2008**, *7*, 158.
(23) Hau, S. K.; Yip, H.-L.; Baek, N. S.; Zou, J.; O'Malley, K.; Jen, A. K.-Y. *Appl. Phys. Lett.* **2008**, *92*, 253301.
(24) Park, Y.; Choong, V.; Gao, Y.; Hsieh, B. R.; Tang, C. W. *Appl. Phys. Lett.* **1996**, *68*, 2699.
(25) Sugiyama, K.; Ishii, H.; Ouchi, Y. *J. Appl. Phys.* **2000**, *87*, 295.
(26) Waldauf, C.; Morana, M.; Denk, P.; Schilinsky, P.; Coakley, K.; Choulis, S. A.; Brabec, C. J. *Appl. Phys. Lett.* **2006**, *89*, 233517.
(27) Tao, C.; Xie, G.; Liu, C.; Zhang, X.; Dong, W.; Meng, F.; Kong, X.; Shen, L.; Ruan, S.; Chen, W. *Appl. Phys. Lett.* **2009**, *95*, 053303.
(28) White, M. S.; Olson, D. C.; Shaheen, S. E.; Kopidakis, N.; Ginley, D. S. *Appl. Phys. Lett.* **2006**, *89*, 143517.
(29) Baek, W. H.; Choi, M.; Yoon, T.-S.; Lee, H. H.; Kim, Y. S. *Appl. Phys. Lett.* **2010**, *96*, 133506.
(30) Li, C. Y.; Wen, T. C.; Lee, T. H.; Guo, T. F.; Huang, J. C. A.; Lin, Y. C.; Hsu, Y. J. *J. Mater. Chem.* **2009**, *19*, 1643.
(31) Kim, J. Y.; Noh, S.; Nam, Y. M.; Kim, J. Y.; Roh, J.; Park, M.; Amsden, J. J.; Yoon, D. Y.; Lee, C.; Jo, W. H. *ACS Appl. Mater. Interfaces* **2011**, *3*, 4279.
(32) Kuwabara, T.; Iwata, C.; Yamaguchi, T.; Takahashi, K. *ACS Appl. Mater. Interfaces* **2010**, *2*, 2254.
(33) Campbell, I. H.; Kress, J. D.; Martin, R. L.; Smith, D. L.; Barashkov, N. N.; Ferraris, J. P. *Appl. Phys. Lett.* **1997**, *71*, 24.
(34) Appleyard, S. F. J.; Day, S. R.; Pickford, R. D.; Willis, M. R. *J. Mater. Chem.* **2000**, *10*, 169.
(35) Khodabakhsh, S.; Poplavskyy, D.; Heutz, S.; Nelson, J.; Bradley, D. D. C.; Murata, H.; Jones, T. S. *Adv. Funct. Mater.* **2004**, *14*, 1205.
(36) Kim, J. S.; Park, J. H.; Lee, J. H.; Jo, J.; Kim, D.-Y.; Cho, K. *Appl. Phys. Lett.* **2007**, *91*, 112111.
(37) Hau, S. K.; Yip, H.-L.; Acton, O.; Baek, N. S.; Ma, H.; Jen, A. K.-Y. *J. Mater. Chem.* **2008**, *18*, 5113.
(38) Zhang, H.; Ouyang, J. *Appl. Phys. Lett.* **2010**, *97*, 063509.
(39) Zhang, H.; Ouyang, J. *Org. Electron.* **2011**, *12*, 1864.
(40) Sun, K.; Zhang, H.; Ouyang, J. *J. Mater. Chem.* **2011**, *21*, 18339.
(41) Hains, A. W.; Chen, H. Y.; Reilly, T. H.; Gregg, B. A. *ACS Appl. Mater. Interfaces* **2011**, *3*, 4381.
(42) Chen, Q.; Worfolk, B. J.; Hauger, T. C.; Al-Atar, U.; Harris, K. D.; Buriak, J. M. *ACS Appl. Mater. Interfaces* **2011**, *3*, 3962.
(43) Seo, J. H.; Namdas, E. B.; Gutacker, A.; Heeger, A. J.; Bazan, G. C. *Appl. Phys. Lett.* **2010**, *97*, 043303 (ion motion).
(44) Lenes, M.; Bolink, H. J. *ACS Appl. Mater. Interfaces* **2010**, *2*, 3664.
(45) Gan, L. M.; Chow, P. Y.; Liu, Z.; Han, M.; Quek, C. H. *Chem. Commun.* **2005**, 4459.
(46) Henningsen, R.; Gale, B. L.; Straub, K. M.; DeNagel, D. C. *Proteomics* **2002**, *2*, 1479.
(47) Yoshizawa, M.; Hirao, M.; Akita, K. I.; Ohno, H. *J. Mater. Chem.* **2001**, *11*, 1057.
(48) Tiyapiboonchaiya, C.; Pringle, J. M.; Sun, J.; Byrne, N.; Howlett, P. C.; MacFarlane, D. R.; Forsyth, M. *Nat. Mater.* **2004**, *3*, 29.

(49) Byrne, N.; Howlett, P. C.; MacFarlane, D. R.; Forsyth, M. *Adv. Mater.* **2005**, *17*, 2497.

(50) Hatanaka, T.; Morigaki, S.; Aiba, T.; Katayama, K.; Koizumi, T. *Int. J. Pharm.* **1995**, *125*, 195.

(51) Mazzenga, G. C.; Berner, B. *J. Controlled Release* **1991**, *16*, 77.

(52) Xia, Y.; Zhang, H.; Ouyang, J. *J. Mater. Chem.* **2010**, *20*, 9740.

(53) Brabec, C. J.; Cravino, A.; Meissner, D.; Sariciftci, N. S.; Fromherz, T.; Rispens, M. T.; Sanchez, L.; Hummelen, J. C. *Adv. Funct. Mater.* **2001**, *11*, 374.

(54) So, S. K.; Choi, W. K.; Cheng, C. H.; Leung, L. M.; Kwong, C. F. *Appl. Phys. A: Mater. Sci. Process.* **1999**, *68*, 447.

(55) Kudo, Y.; Kusabiraki, M. *Jpn. J. Appl. Phys.* **2006**, *45*, 8517.

(56) Khodabkhsh, S.; Sanderson, B. M.; Nelson, J.; Jones, T. S. *Adv. Funct. Mater.* **2006**, *16*, 95.

(57) Bardecker, J. A.; Ma, H.; Kim, T.; Huang, F.; Liu, M. S.; Cheng, Y.-J.; Ting, G.; Jen, A. K.-Y. *Adv. Funct. Mater.* **2008**, *18*, 3964.

(58) Hotchkiss, P. J.; Li, H.; Paramonov, P. B.; Paniagua, S. A.; Jones, S. C.; Armstrong, N. R.; Brédas, J.-L.; Marder, S. R. *Adv. Mater.* **2009**, *21*, 4496.

(59) Guthrie, J. P. *Can. J. Chem.* **1978**, *56*, 2342.